Polymer Chemistry

ROYAL SOCIETY OF CHEMISTRY

PAPER

View Article Online
View Journal

Cite this: DOI: 10.1039/d6py00089d

Fluorescently labelled polypropylene as a model microplastic for cellular imaging

Alexander Evans, †[a] Ríona M. Devereux, †[a] Zoë R. Turner, [a] Angela J. Russell *[a,b] and Dermot O'Hare *[a]

Polypropylene (PP) is the second most produced plastic globally and is environmentally pervasive in the form of microplastics (MPs). The cellular localisation and fate of MPs within biological systems remain poorly understood. We present a method for the covalent functionalisation of PP with the fluorescent label rhodamine B (**Rb**) and its subsequent MP evaluation in a human embryonic kidney model cell line (HEK293T). **Rb** was successfully coupled into PP ($\mathbf{PP_{Rb}}$) under Steglich esterification conditions. $\mathbf{PP_{Rb}}$ is stable under physiological pH and so can be utilised *in vitro*, offering a significantly improved MP model for conventional staining methods that can definitively locate MPs in human cells. Cellular uptake of $\mathbf{PP_{Rb}}$ was rapid (≤1 h), and $\mathbf{PP_{Rb}}$ was non-toxic up to 70 μM and was not observed to localise within the nucleus. Increased mean lysosomal fluorescence intensity suggested an endosomal uptake mechanism followed by significant clearance over a 48 h period. This approach provides a robust platform for definitive microplastic tracking, enabling reliable, standardised studies of polymer–cell interactions across biological systems.

Received 28th January 2026,
Accepted 26th March 2026

DOI: 10.1039/d6py00089d

rsc.li/polymers

Introduction

Commercially, polyolefins (PO), namely polypropylene (PP)[1] and polyethylene (PE),[2] are synthesised at scale to meet the needs of a broad array of applications, with PP accounting for 17% of global plastic production.[3] Desirable and tuneable properties, such as mechanical strength or creep resistance, as a result of branching, molecular mass (M_n), and dispersities ($Đ_M$), coupled with low production costs are amongst the driving forces behind their widespread utility.[4] Although PP is recyclable, a significant proportion enters landfills or the environment.[5–7] A large amount of PP waste is converted to microplastics (MPs),[8] or indeed nanoplastics,[9] *via* slow degradation due to (a)biotic factors.[7] Detection of PO MPs is widely reported, and they are highly prevalent.[10,11] Plastic debris is an environmentally persistent and complex contaminant (*e.g.* varying in size, morphology, and chemical constituency),[12] whilst MP detection remains challenging.[13,14] Consequently, recent legislative efforts have been introduced in Europe to curtail the prevalence of single use plastics, given the emergence of MPs as a pressing environmental concern due to their ubiquity, potential ecological ramifications, and associated risk.[10,14–17]

The impact of MPs on macroscopic organisms has been extensively studied, with recent reports evaluating their effects on mice,[18,19] fish,[20–22] and humans.[23] There are reports detailing MP entry into aquatic and terrestrial food chains *via* biomagnification and bioaccumulation,[12,24–26] and their detection in fish, birds, and mammals feeding on aquatic organisms or living in aquatic environments has been the subject of further investigation.[22,27] Perturbation of ecological processes may align with other anthropogenic pollutants despite the lack of lethality; reduced fecundity and growth at the first trophic level may cause persistent reduction of biomass.[28,29] Additionally, investigations into which animals can ingest MPs and the mechanism by which this occurs have been reported.[30,31] However, the marked chemical inertness severely hampers evaluation on living species; the incorporation of a fluorescent probe circumvents MP detection issues in organic tissues.[32–37]

However, the effects on single-celled organisms, which constitute fundamental components of aquatic ecosystems, remain relatively underexplored. These minute organisms, encompassing diverse taxa such as phytoplankton and protozoa, play pivotal roles in nutrient cycling and food web dynamics.[29,38–40] The ingestion of microplastics by single-celled organisms can lead to various detrimental outcomes, including altered feeding behaviours, impaired metabolic functions, and compromised reproductive success.[29,38–40] Furthermore, the sorption of toxic chemicals onto microplastics introduces an additional layer of risk, as the bioavailability of these pollutants increases upon ingestion by these microorganisms,[13,16,28,33,41] although disputed.[10] Despite the limited research in this area, the potential for cascading effects throughout aquatic ecosystems underscores the urgency to comprehensively elucidate the consequences of

[a]*Chemistry Research Laboratory, Department of Chemistry, University of Oxford, 12 Mansfield Road, OX1 3TA Oxford, UK. E-mail: dermot.ohare@chem.ox.ac.uk, angela.russell@chem.ox.ac.uk*
[b]*Department of Pharmacology, University of Oxford, Mansfield Road, OX1 3QT, Oxford, UK*
† These authors contributed equally to this work.

microplastic exposure on single-celled organisms. Ascertaining an understanding of the posed risk is crucial for the educated development of policy. Current methods for evaluating the role of MPs with single-celled organisms predominantly utilise staining,[42] due to the relative synthetic simplicity,[43] although some dyes are covalently bound.[37] *In vitro* assays on mice[44] and human[45] cell lines utilise polystyrene (PS) for this purpose. However, this methodology has drawbacks, primarily leaching of free dye, potentially leading to the presence of artefacts, confounding the interpretation of the results.[46–48] Subsequently, reports with claims of polymer sample purity, or indeed covalent coupling of dye units to the polymer chain, are not supported by adequate rigorous characterisation data leading to the ambiguous interpretation of results.

In the field of mechanical recycling, separation techniques have been extended to include fluorescent labelling, enabling separation by specific polymeric materials;[49–51] recent reports utilise fluorescently tagged PE in this way.[52] Notably, the recycling process typically involves high temperatures and consequently careful selection of incorporated spectroscopic markers is required to avoid degradation.[52] To the best of our knowledge, the recent literature presents a few examples of synthesised *isotactic*-PP copolymers containing fluorescent units, and, so far, only the work by Pragliola *et al.* has evaluated them as a fluorescent marker of PP.[32,53] Fluorescent probe coupled PP may be used to mimic the *in vivo* behaviour of PP-derived MP pollutants on a cellular level.

Several Norwegian institutions and initiatives have pioneered extensive studies in evaluating MP research;[54] despite a plethora of published articles, it is posited that a lack of standardisation and validated methods, particularly for the smallest plastic particles, hampers conclusive and harmonised research.[55] Given the interdisciplinary nature of the problem, it is well within the remit of polymer scientists to design, synthesise, and provide specific model polymers for MP analysis in collaboration with relevant academic disciplines. We have recently reported a general two-step methodology to functionalise PP, creating a wide range of covalent linkages, something traditionally difficult to achieve in a controlled manner.[56] Consequently, we present a method for the covalent fluorescent labelling of rhodamine B (**Rb**) functionalised PP, $\mathbf{PP_{Rb}}$, and subsequent MP evaluation in a human kidney cell line. We believe that this work provides a new methodology for covalently bound fluorescent tags on a PO system which allows confident analysis of any polymer–cell interaction. This has the potential to offer a harmonised approach for the study of related polymeric materials and enable conclusive evaluation of the interaction of such ubiquitous materials within cells and organisms.

Results and discussion

Synthesis and characterisation of $\mathbf{PP_{Rb}}$

$\mathbf{PP_{Rb}}$ was synthesised *via* the quantitative transformation of a previously reported alcohol-functionalised PP copolymer ($\mathbf{PP_{EAE}}$) under Steglich esterification conditions (DMAP 0.3 eq., DCC 2 eq., DCM, 80 °C, 72 h) with **Rb** (2 eq.) (Fig. 1).[56,57]

Following extensive purification by water Soxhlet extraction, $\mathbf{PP_{Rb}}$ with 1.87 mol% covalently-bound dye incorporation was isolated and fully characterised. Key ^{1}H NMR spectroscopic handles evidence the presence of the dye; six aromatic resonances between 6.37 and 7.91 ppm integrate appropriately (Fig. S1). Convection compensated diffusion experiments support the conclusion that **Rb** is bound to a higher molecular weight species with a diffusion coefficient of 9.8×10^{-6} cm^2 s^{-1} (Fig. 1E), which is comparable to the parent copolymer (*ca.* 9.9×10^{-6} cm^2 s^{-1}) and considerably different from the free dye (*ca.* 6.2×10^{-6} cm^2 s^{-1}) as tracked by aromatic protons and a distinct quartet assigned to –NC$\boldsymbol{H}_2$CH$_3$ (3.44 ppm) (Fig. S1 and S2). $\mathbf{PP_{Rb}}$ solution in chloroform (0.5 mg mL^{-1}) exhibits an excitation wavelength (λ_{Ex}) of 558 nm by ultraviolet–visible (UV-Vis) spectroscopy (Fig. 1B). Significantly, the polymer was also shown to be fluorescent with an emission wavelength (λ_{Em}) of 581 nm (Fig. 1C). Crucially, λ_{Ex} and λ_{Em} are distinctly altered when compared to derivative **Rb** (λ_{Ex} = 569 nm, λ_{Em} = 592 nm) in a comparable molar concentration of the fluorophore in chloroform (Fig. S8).

The polymer was further characterised by Fourier transform infrared spectroscopy (ν = 1736 cm^{-1} (C═O) and 808 cm^{-1} (C═C$_{Ar}$)) and differential scanning calorimetry (T_m = 113 °C), and a single decomposition step was evidenced (T_{max} = 431 °C) by thermogravimetric analysis (Fig. S6). Multiple complementary techniques were employed to assess the polymer particle size, as variations in measurement conditions can substantially influence the observed dimensions. M_n analysis by size exclusion chromatography (SEC) was unsuccessful, with $\mathbf{PP_{Rb}}$ not eluting within the calibration window; however, the theoretical molar mass ($M_{n,\,th}$) is predicted to be *ca.* 14 700 g mol^{-1} based on the parent copolymer experimental molar mass ($M_{n,\,SEC}$ = 13 800 g mol^{-1}) (Fig. S6). Since the Mark–Houwink correlation is not known for functionalized PP, and the presence of a polar group is likely to affect the radius of gyration in solution, it is reasonable to assume that the backbone chain length remains unchanged during post polymerization modification.[58] Dynamic light scattering (DLS) suggests that $\mathbf{PP_{Rb}}$ aggregates in the solution state, common for amphiphilic copolymers and potentially induced by the ionic nature of the fluorophore.[59] $\mathbf{PP_{Rb}}$ in toluene solution (1 mg mL^{-1}) exhibited good agreement between number, volume, and intensity values for the hydrodynamic diameter (D_h), *ca.* 570 nm, which increased from that of the parent copolymer, *ca.* 140 nm, supporting a micellar arrangement in solution with increasing hydrophilic character (Fig. 1D, Fig. S7, and Table S1). It is worth noting that this may subsequently affect the permeability of $\mathbf{PP_{Rb}}$ towards the cell membrane; however, existing *in vitro* experiments employ charged, colloidally stable PS particles[44] and we believe that our approach offers an alternative with significantly reduced impact (*vide infra*). Additionally, some $\mathbf{PP_{Rb}}$ was cryofractured ($^{c}\mathbf{PP_{Rb}}$) in an attempt to simulate accelerated weathering (Fig. S9 and S10), such that the irregularities in size and shape of MPs found within the environment could be rudimentarily assessed.[32]

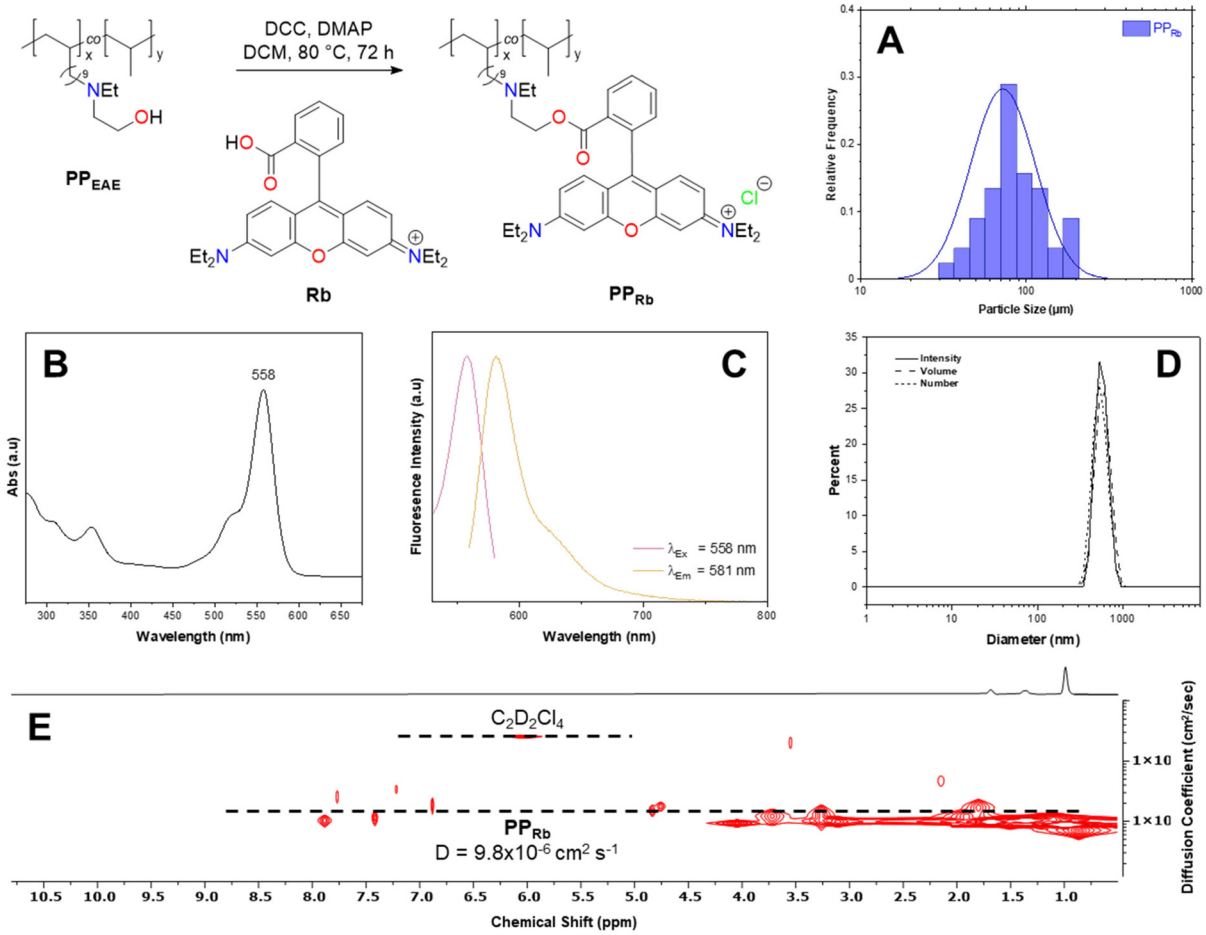

Fig. 1 Scheme: synthesis of PP_{Rb} under Steglich esterification conditions, (A) solid particle size distribution histogram as determined by SEM (Fig. S9), (B) UV-Vis spectrum of PP_{Rb} solution (0.5 mg mL^{-1}, chloroform), (C) fluorescence spectrum of PP_{Rb} solution (0.5 mg mL^{-1}, chloroform), (D) DLS analysis of PP_{Rb} solution (1 mg mL^{-1}, toluene), and (E) DOSY ^{1}H NMR spectrum (500 MHz, $C_2D_2Cl_4$, 393 K) of PP_{Rb}.

Cellular studies

Incorporating fluorophores directly into MP models marks a critical advancement in visualising and understanding MP interactions within biological systems. Fluorophore incorporation on PP enabled an *in vitro* investigation in a human embryonic kidney (HEK293T) model cell line, where PP_{Rb} is utilised as a model for MPs, overcoming imaging issues suffered by traditional polyolefins. Through the covalent linkage of the dye moiety, it can be concluded that any observations arise due to the presence of the dye-bound polymer and not through leaching; other methods previously reported suffer from this drawback.[42,48,60] A control experiment was performed to measure polymer–dye stability using a citrate–phosphate buffer solution, mimicking the acidic lysosomal compartments (pH 4, 38 °C), as detailed in the SI.[61] Detected fluorescence correlated to a maximum hydrolysis of 1.6% over 3 days, and was deemed not statistically significant, suggesting minimal degradation in a physiologically relevant pH range (Fig. S17).

HEK293T cells were chosen as the model cell line to investigate uptake and localisation *via* confocal microscopy. The primary entry points for MPs into the human body are ingestion, inhalation, and dermal contact.[62,63] Once internalised, MPs can enter the circulatory system, potentially accumulating in organs such as the gut, liver, and kidneys.[64] Given the kidney's role in filtering and detoxifying various substances, including environmental contaminants like MPs, the HEK293T cell line serves as a relevant model for examining cellular defence mechanisms in response to MPs.[65]

The acute cytotoxicity of PP_{Rb} was assessed *in vitro* using the AlamarBlue™ Cell Viability Assay in HEK293T cells. Cells were exposed to a range of [PP_{Rb}] for 24 h, with cell viability measured across the concentration gradient. No significant cytotoxic effects were observed up to the highest concentration tested (PP_{Rb} = 70 μM), as compared to the control group (PP_{Rb} = 0 μM) (Fig. 2). Additionally, bright-field microscopy of cells treated with 35 μM PP_{Rb} for 24 h revealed no signs of cell death or structural abnormalities relative to untreated control cells (Fig. 2 and S13). It is worth noting that PP_{Rb} was rigorously purified prior to cellular treatment. In environmental contexts, however, MPs often act as sorbents, potentially concentrating harmful and toxic

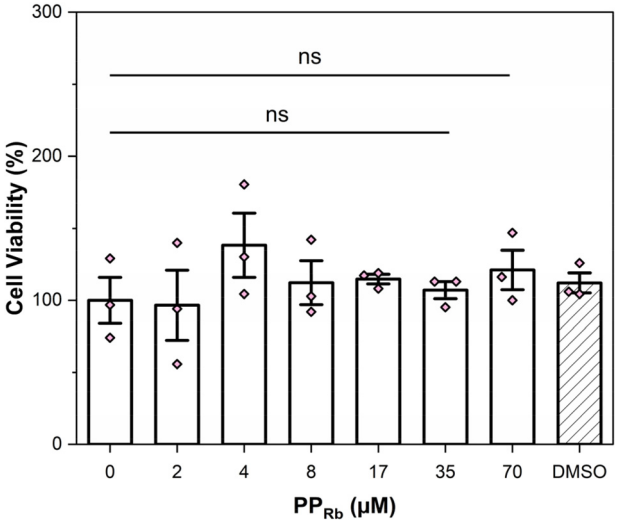

Fig. 2 *In vitro* cytotoxicity assessment of PP_{Rb} in HEK293 cells using the AlamarBlue™ Cell Viability Assay. Cell viability (%) in response to various concentrations of PP_{Rb} (0–70 μM) after 24 h of treatment, as compared to the DMSO control group. Data are presented as mean ± standard error of the mean (n = 3). Brown–Forsythe and Welch one-way ANOVA, non-parametric (ns = p > 0.05).

materials on their surfaces, which may influence their biological effects.[33,66–68]

To assess the uptake and localisation of $\mathbf{PP_{Rb}}$ *in vitro*, HEK293T cells were incubated with either 35 μM of unbound fluorophore (**Rb**) or fluorophore-bound $\mathbf{PP_{Rb}}$ for 1 h and compared with untreated control cells (Fig. 3). A detectable signal was observed in the 555 nm channel for both **Rb** and $\mathbf{PP_{Rb}}$, with minimal background fluorescence in the negative control group. Notably, cells treated with $\mathbf{PP_{Rb}}$ exhibited a higher signal intensity compared to those treated with free **Rb**, indicating a consistent cellular uptake of $\mathbf{PP_{Rb}}$ without removal upon washing. The 1 h treatment period demonstrates rapid cellular uptake and accumulation of $\mathbf{PP_{Rb}}$ within HEK293T cells. The dye-bound polymer, $\mathbf{PP_{Rb}}$, exhibits localisation within cells due to its polymeric structure, in contrast to the free **Rb** dye, which results in a more diffuse cellular distribution. Accumulation of $\mathbf{PP_{Rb}}$ within cells was evident, as confirmed by z-stack imaging (Fig. 3), highlighting the polymer's capacity for localised uptake and retention compared with the less structured, widespread localisation pattern observed with free **Rb**. The different observed cellular behaviours of both **Rb** and $\mathbf{PP_{Rb}}$ are consistent with the absence of ester hydrolysis and dye liberation from $\mathbf{PP_{Rb}}$ (Fig. S17).[69]

After 24 h, cellular localisation of $\mathbf{PP_{Rb}}$ is reduced compared to the 1 h time point, suggesting a potential decrease in intracellular retention (Fig. 4B). This reduction in cellular localisation may indicate that $\mathbf{PP_{Rb}}$ is being actively removed from the cell through a cellular clearance pathway, possibly *via* an endosomal recycling pathway, although a metabolic degradation pathway cannot be ruled out.[70]

A competition assay was conducted to assess the influence of the parent alcohol-functionalised copolymer, $\mathbf{PP_{EAE}}$, on the cellular localisation of $\mathbf{PP_{Rb}}$ after 24 h (Fig. 4A and B). The results indicated that the parent polymer directs cellular localisation of $\mathbf{PP_{Rb}}$, as fluorescence was significantly decreased upon co-incubation with 35 μM $\mathbf{PP_{EAE}}$. In contrast, the localisation of **Rb** remained unaffected by the presence of $\mathbf{PP_{EAE}}$, supporting the conclusion that $\mathbf{PP_{EAE}}$ and $\mathbf{PP_{Rb}}$ localise to the same cellular compartments, while **Rb** does not. This further supports the limited impact of the charged fluorophore driving cellular uptake, trafficking and compartmentalisation, strengthening the role of $\mathbf{PP_{Rb}}$ as a model MP. Notably, this competitive reduction in fluorescence was not observed with the **Rb** fluorophore alone, underscoring that $\mathbf{PP_{EAE}}$, and not **Rb**, modulates the intracellular dynamics of $\mathbf{PP_{Rb}}$ localisation.

Furthermore, a sample of $\mathbf{PP_{Rb}}$ was subjected to cryogenic fracturing to produce $\mathbf{^{c}PP_{Rb}}$, a model intended to simulate accelerated environmental degradation.[32] However, data showed no significant difference in cellular localisation between $\mathbf{^{c}PP_{Rb}}$ and the original $\mathbf{PP_{Rb}}$ sample (Fig. S11). Importantly, across all timepoints, there was no detectable co-localisation of $\mathbf{PP_{Rb}}$ and the nuclear stain DAPI (Fig. S11).

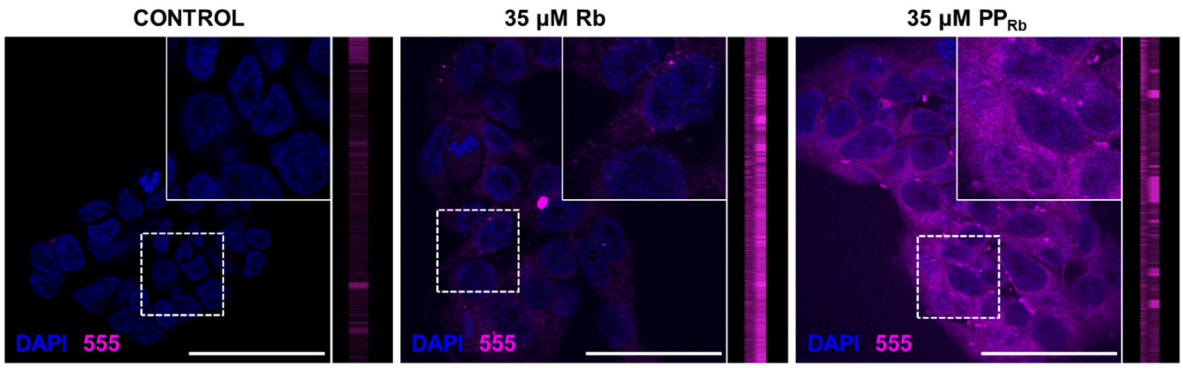

Fig. 3 Confocal microscopy images showing the cellular localisation of the dye-bound polymer PP_{Rb} and free **Rb** in HEK293T cells. Cells were incubated with either 35 μM of free **Rb** or PP_{Rb} for 1 h and compared with untreated control cells. The images show fluorescence representing the presence of **Rb** or PP_{Rb} (magenta) and DAPI nuclear staining (blue). The inset (top right) presents a (2×) zoomed-in view highlighting the compartmentalisation of **Rb** or PP_{Rb}. Z-stack panels (side view) illustrate the spatial distribution of fluorescence within the cells. Scale bars = 50 μm.

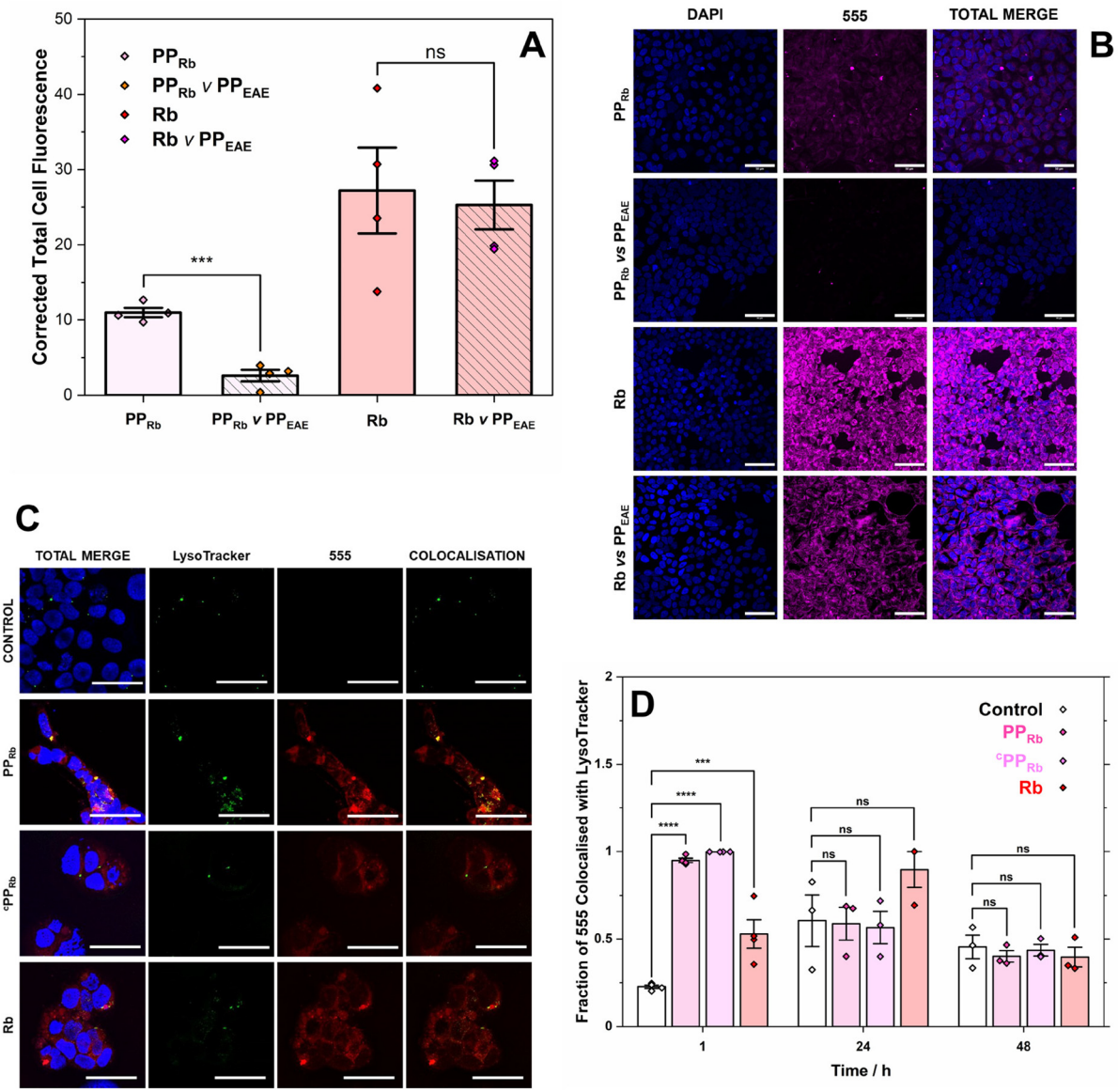

Fig. 4 (A/B) Comparison of corrected total cell fluorescence at 555 nm for $\mathbf{PP_{Rb}}$, the competition condition ($\mathbf{PP_{Rb}}$ *vs.* $\mathbf{PP_{EAE}}$), free **Rb**, and **Rb** co-incubated with $\mathbf{PP_{EAE}}$ (**Rb** *vs.* $\mathbf{PP_{EAE}}$) in a fluorescence competition experiment at the 24 h timepoint (n = 3). (A) Quantification showing a significant reduction in fluorescence for the competition condition $\mathbf{PP_{Rb}}$ *vs.* $\mathbf{PP_{EAE}}$ compared to $\mathbf{PP_{Rb}}$, indicating that fluorescent localisation is outcompeted by the parent compound $\mathbf{PP_{EAE}}$ at 24 h. The fluorescence of free **Rb** remains unchanged with cotreatment with $\mathbf{PP_{EAE}}$ (**Rb** *vs.* $\mathbf{PP_{EAE}}$). (B) Confocal microscopy images showing nuclear staining with DAPI (blue), **Rb** fluorescence (555 nm), and merged channels for $\mathbf{PP_{Rb}}$, $\mathbf{PP_{Rb}}$ *vs.* $\mathbf{PP_{EAE}}$, **Rb**, and **Rb** *vs.* $\mathbf{PP_{EAE}}$ conditions at the 24 h timepoint. Scale bars 50 μm. (C/D) Quantification of colocalization of $\mathbf{PP_{Rb}}$, $\mathbf{^cPP_{Rb}}$, and free **Rb** with lysosomes in HEK293T cells at various time points. (C) Confocal microscopy images showing lysosomal staining with LysoTracker (green), nuclear staining with DAPI (blue) and 555 channel (red) in control cells and cells treated with 35 μM of $\mathbf{PP_{Rb}}$, $\mathbf{^cPP_{Rb}}$, or free **Rb** for 1 h. Scale bars = 50 μm. (D) The fraction of 555 colocalization with LysoTracker was quantified for each treatment group (see also Fig. S14 and S15). (A/D) Data are presented as mean ± standard error of the mean (n = 3). Brown–Forsythe and Welch one-way ANOVA, non-parametric (***p < 0.001, ****p < 0.0001, and ns = p > 0.05 compared to the control).

Excluding certain molecules or structures from the nucleus can prevent potential disruptions to nuclear architecture or DNA stability, safeguarding essential cellular processes.[71]

It was hypothesised that, due to the polymer size and relatively low M_n, the polymer, or any nanoparticles formed through self-assembly, would enter the cells through an energy-dependent trafficking mechanism *via* an endosomal pathway.[72] It is, therefore, reasonable to infer possible trafficking of $\mathbf{PP_{Rb}}$ to the lysosomes upon cellular entry. To investigate this, HEK293T cells were stained with LysoTracker, an acidic vesicle-labelling dye, and incubated with $\mathbf{PP_{Rb}}$ for 1, 24, and 48 h (Fig. 4C, S14–S16). The mean LysoTracker fluorescence intensity for $\mathbf{PP_{Rb}}$, $\mathbf{^cPP_{Rb}}$ and free **Rb** increased relative to the control at 1 and 24 h, suggesting a potential endosomal uptake

mechanism. By 48 h, however, the mean fluorescence intensity of LysoTracker in the $\mathbf{PP_{Rb}}$ and $^{c}\mathbf{PP_{Rb}}$ treated cells returned to control levels, while the fluorescence for free **Rb** remained elevated. Following this, the colocalization of the 555 channels with LysoTracker was investigated for $\mathbf{PP_{Rb}}$, $^{c}\mathbf{PP_{Rb}}$, and **Rb** (Fig. 4C and D and S14 and S15). Incubation of $\mathbf{PP_{Rb}}$ and $^{c}\mathbf{PP_{Rb}}$ showed a significant fraction of channel overlap at 1 h, confirming colocalization of the polymer with lysosomes *in vitro* at this early timepoint. However, this overlap was insignificant at the 24 and 48 h timepoints. These colocalization results further support a lysosomal uptake mechanism. Free **Rb** showed no significant overlap at all tested timepoints, suggesting that the increase in lysosomes may not be directly associated with free **Rb** and could be a secondary effect of its incubation. These observations and earlier dosing data showing reduced $\mathbf{PP_{Rb}}$ uptake by 24 h (Fig. 4B) suggest that cells may actively work to clear the polymer over time.

Concluding remarks

Polypropylene with the covalently-bound fluorescent rhodamine B tag, $\mathbf{PP_{Rb}}$, was synthesised and characterised for *in vitro* studies against a HEK293T cell line and evaluated by confocal microscopy. The two-step copolymerization–post-modification strategy employed is facile and, importantly, allows the preparation of rigorously purified model polymer samples that do not undergo dye leaching.

Incubation with $\mathbf{PP_{Rb}}$ resulted in rapid cellular uptake (1 h) whilst remaining non-toxic up to 70 μM. Crucially, no localisation within the nucleus was observed under the limits of detection. Initial investigations were undertaken into the uptake mechanism and efficacy as a PP MP model. Increased mean lysosomal fluorescence intensity following $\mathbf{PP_{Rb}}$ treatment suggests an endosomal uptake mechanism with significant clearance implied over a 48 h period. Cellular localisation of $\mathbf{PP_{Rb}}$ is directed by the parent alcohol-functionalised copolymer, as evidenced by competition studies, indicating that $\mathbf{PP_{Rb}}$ is a valuable model for PP cell interaction. Optimistically, accounting for the constraints of our investigation, $\mathbf{PP_{Rb}}$ acts as an inert orthogonal species within the cell. However, it is important to investigate this further, especially by probing the polymer species as a vector for harmful environmental substances.

We believe that this method for the synthesis and application of covalently bound dye moieties can elucidate the degree to which concern can be levied against the developing environmental plastic pollution. More broadly, this blueprint can enable a precise and confident interlaboratory analysis of polymer–cell interactions through the targeted synthesis of dye-modified polymers of interest. Additionally, this method offers many investigative opportunities, be it an *in vitro* cell line or *in vivo* studies of more complex organisms, including their ecological surroundings.

Author contributions

A. E. performed the investigation and formal analysis of polymer-related experiments. R. M. D. undertook the investigation and formal analysis of biological-related experiments. A. E. conceived and managed the project and drafted the manuscript. All authors revised the manuscript. D. O. H. and A. J. R. supervised the research and acquired the funding.

Conflicts of interest

There are no conflicts to declare.

Data availability

The supporting data have been provided as part of the supplementary information (SI). Supplementary information: experimental and data analysis methods, supporting polymer characterization, and images and data pertaining to the cell studies. See DOI: https://doi.org/10.1039/d6py00089d.

Acknowledgements

A. E. thanks the EPSRC for funding under the Impact Acceleration Awards Doctoral Impact Scheme. The research reported in this work was (in part) supported financially by SCG Chemicals PLC (Thailand). R. M. D. thanks Wellcome Trust (218514/Z/19/Z) for studentship funding, established with support from Merck Sharp and Dohme Corp and Janssen Pharmaceutica NV. We also thank Dr Coral Mycroft (Oxford NMR Submission Service) for running various NMR experiments and Ms Liv Thobru, Ms Sara Rund Herum, and Ms Rita Jenssen (Norner AS) for running GPC analysis.

References

1 G. Natta, P. Pino, P. Corradini, F. Danusso, E. Mantica, G. Mazzanti and G. Moraglio, *J. Am. Chem. Soc.*, 1955, **77**, 1708–1710.
2 K. Ziegler, E. Holzkamp, H. Breil and H. Martin, *Angew. Chem.*, 1955, **67**, 426.
3 A. H. Westlie, E. Y.-X. Chen, C. M. Holland, S. S. Stahl, M. Doyle, S. R. Trenor and K. M. Knauer, *Macromol. Rapid Commun.*, 2022, **43**, 2200492.
4 L. Resconi, L. Cavallo, A. Fait and F. Piemontesi, *Chem. Rev.*, 2000, **100**, 1253–1346.
5 R. Francis, *Recycling of Polymers: Methods, Characterization and Applications*, John Wiley & Sons, 2016.
6 V. V. Narmadha, J. Jose, S. Patil, M. O. Farooqui, B. Srimuruganandam, S. Saravanadevi and K. Krishnamurthi, *Int. J. Environ. Res.*, 2020, **14**, 629–640.
7 M. Potrykus, V. Redko, K. Głowacka, A. Piotrowicz-Cieślak, P. Szarlej, H. Janik and L. Wolska, *Sci. Total Environ.*, 2021, **758**, 143649.
8 J. P. G. L. Frias and R. Nash, *Mar. Pollut. Bull.*, 2019, **138**, 145–147.

9 J. Gigault, A. T. Halle, M. Baudrimont, P. Y. Pascal, F. Gauffre, T. L. Phi, H. El Hadri, B. Grassl and S. Reynaud, *Environ. Pollut.*, 2018, **235**, 1030–1034.
10 E. E. Burns and A. B. A. Boxall, *Environ. Toxicol. Chem.*, 2018, **37**, 2776–2796.
11 J. Sun, X. Dai, Q. Wang, M. C. M. van Loosdrecht and B.-J. Ni, *Water Res.*, 2019, **152**, 21–37.
12 A. A. Horton, A. Walton, D. J. Spurgeon, E. Lahive and C. Svendsen, *Sci. Total Environ.*, 2017, **586**, 127–141.
13 S. O. Fakayode, T. F. Mehari, V. E. Fernand Narcisse, C. Grant, M. E. Taylor, G. A. Baker, N. Siraj, M. Bashiru, I. Denmark, A. Oyebade, D. K. Bwambok, C. Kuedukey, T. Alonge and D. Anum, *Appl. Spectrosc. Rev.*, 2024, **59**, 1183–1277.
14 G. Chen, Q. Feng and J. Wang, *Sci. Total Environ.*, 2020, **703**, 135504.
15 A. A. Koelmans, P. E. Redondo-Hasselerharm, N. H. M. Nor, V. N. de Ruijter, S. M. Mintenig and M. Kooi, *Nat. Rev. Mater.*, 2022, **7**, 138–152.
16 P. Liu, X. Zhan, X. Wu, J. Li, H. Wang and S. Gao, *Chemosphere*, 2020, **242**, 125193.
17 K. Liu, X. Wang, T. Fang, P. Xu, L. Zhu and D. Li, *Sci. Total Environ.*, 2019, **675**, 462–471.
18 Y. Jin, L. Lu, W. Tu, T. Luo and Z. Fu, *Sci. Total Environ.*, 2019, **649**, 308–317.
19 L. Lu, Z. Wan, T. Luo, Z. Fu and Y. Jin, *Sci. Total Environ.*, 2018, **631–632**, 449–458.
20 L. Lei, S. Wu, S. Lu, M. Liu, Y. Song, Z. Fu, H. Shi, K. M. Raley-Susman and D. He, *Sci. Total Environ.*, 2018, **619–620**, 1–8.
21 A. Batel, F. Linti, M. Scherer, L. Erdinger and T. Braunbeck, *Environ. Toxicol. Chem.*, 2016, **35**, 1656–1666.
22 L. C. de Sá, M. Oliveira, F. Ribeiro, T. L. Rocha and M. N. Futter, *Sci. Total Environ.*, 2018, **645**, 1029–1039.
23 N. Chartres, C. B. Cooper, G. Bland, K. E. Pelch, S. A. Gandhi, A. BakenRa and T. J. Woodruff, *Environ. Sci. Technol.*, 2024, **58**(52), 22843–22864.
24 Y. Huang, Q. Liu, W. Jia, C. Yan and J. Wang, *Environ. Pollut.*, 2020, **260**, 114096.
25 F. S. Hamid, M. S. Bhatti, N. Anuar, N. Anuar, P. Mohan and A. Periathamby, *Waste Manage. Res.*, 2018, **36**, 873–897.
26 A. A. de Souza Machado, W. Kloas, C. Zarfl, S. Hempel and M. C. Rillig, *Glob. Chang. Biol.*, 2018, **24**, 1405–1416.
27 N. Baranzini, L. Pulze, C. Bon, L. Izzo, S. Pragliola, V. Venditto and A. Grimaldi, *Fish Shellfish Immunol.*, 2022, **127**, 492–507.
28 T. S. Galloway, M. Cole and C. Lewis, *Nat. Ecol. Evol.*, 2017, **1**, 0116.
29 P. Raju, P. Santhanam, S. S. Pandian, M. Divya, A. Arunkrishnan, K. N. Devi, S. Ananth, J. Roopavathy and P. Perumal, *Arch. Microbiol.*, 2021, **204**, 84.
30 S. Anbumani and P. Kakkar, *Environ. Sci. Pollut. Res.*, 2018, **25**, 14373–14396.
31 H. S. Auta, C. U. Emenike and S. H. Fauziah, *Environ. Int.*, 2017, **102**, 165–176.
32 S. Pragliola, F. Grisi, V. Vitale, O. Sacco, V. Venditto, L. Izzo, A. Grimaldi and N. Baranzini, *Polym. Chem.*, 2022, **13**, 2685–2693.
33 C. Campanale, C. Massarelli, I. Savino, V. Locaputo and V. F. Uricchio, *Int. J. Environ. Res. Public Health*, 2020, **17**, 1212.
34 T. Maes, R. Jessop, N. Wellner, K. Haupt and A. G. Mayes, *Sci. Rep.*, 2017, **7**, 44501.
35 L. Nalbone, A. Panebianco, F. Giarratana and M. Russell, *Mar. Pollut. Bull.*, 2021, **172**, 112888.
36 E. G. Karakolis, B. Nguyen, J. B. You, P. J. Graham, C. M. Rochman and D. Sinton, *Environ. Sci. Technol.*, 2018, **5**, 62–67.
37 B. Nguyen and N. Tufenkji, *Environ. Sci. Technol.*, 2022, **56**, 6426–6435.
38 S. Rist, A. Baun and N. B. Hartmann, *Environ. Pollut.*, 2017, **228**, 398–407.
39 M. Long, I. Paul-Pont, H. Hégaret, B. Moriceau, C. Lambert, A. Huvet and P. Soudant, *Environ. Pollut.*, 2017, **228**, 454–463.
40 Y. Mao, H. Ai, Y. Chen, Z. Zhang, P. Zeng, L. Kang, W. Li, W. Gu, Q. He and H. Li, *Chemosphere*, 2018, **208**, 59–68.
41 M. Gao, Y. Liu and Z. Song, *Chemosphere*, 2019, **237**, 124482.
42 E. G. Karakolis, B. Nguyen, J. B. You, C. M. Rochman and D. Sinton, *Environ. Sci. Technol.*, 2019, **6**, 334–340.
43 S. Morgana, B. Casentini, V. Tirelli, F. Grasso and S. Amalfitano, *Trends Anal. Chem.*, 2024, **172**, 117559.
44 B.-K. Jung, S.-W. Han, S.-H. Park, J.-S. Bae, J. Choi and K.-Y. Ryu, *Neurotoxicology*, 2020, **81**, 189–196.
45 Y. Zhang, S. Wang, V. Olga, Y. Xue, S. Lv, X. Diao, Y. Zhang, Q. Han and H. Zhou, *Chemosphere*, 2022, **291**, 132714.
46 M. T. Sturm, E. Myers, D. Schober, A. Korzin and K. Schuhen, *Analytica*, 2023, **4**, 27–44.
47 W. J. Shim, S. H. Hong and S. E. Eo, *Anal. Methods*, 2017, **9**, 1384–1391.
48 G. Malafaia, T. M. d. Luz, M. A. I. Ahmed, S. Karthi and A. P. d. C. Araújo, *J. Hazard. Mater. Adv.*, 2022, **6**, 100054.
49 D. Jubinville, E. Esmizadeh, S. Saikrishnan, C. Tzoganakis and T. Mekonnen, *Sustainable Mater. Technol.*, 2020, **25**, e00188.
50 E. Maris, A. Aoussat, E. Naffrechoux and D. Froelich, *Miner. Eng.*, 2012, **29**, 77–88.
51 S. Brunner, P. Fomin and C. Kargel, *Waste Manage.*, 2015, **38**, 49–60.
52 A. Arenas-Vivo, F. R. Beltrán, V. Alcázar, M. U. de la Orden and J. Martinez Urreaga, *Mater. Today Commun.*, 2017, **12**, 125–132.
53 R. Shang, H. Gao, F. Luo, Y. Li, B. Wang, Z. Ma, L. Pan and Y. Li, *Macromolecules*, 2019, **52**, 9280–9290.
54 A. L. Lusher, R. Hurley, H. P. H. Arp, A. M. Booth, I. L. N. Bråte, G. W. Gabrielsen, A. Gomiero, T. Gomes, B. E. Grøsvik, N. Green, M. Haave, I. G. Hallanger, C. Halsband, D. Herzke, E. J. Joner, T. Kögel, K. Rakkestad, S. B. Ranneklev, M. Wagner and M. Olsen, *Environ. Int.*, 2021, **157**, 106794.

55 A. Bakir, A. R. McGoran, B. Silburn, J. Russell, H. Nel, A. L. Lusher, R. Amos, R. S. Shadrack, S. J. Arnold, C. Castillo, J. F. Urbina, E. Barrientos, H. Sanchez, K. Pillay, L. Human, T. Swartbooi, M. R. Cordova, S. Y. Sani, T. W. A. W. Wijesinghe, A. A. D. Amarathunga, J. Gunasekara, S. Somasiri, K. Mahatantila, S. Liyanage, M. Müller, Y. Y. Hee, D. F. Onda, K. M. Jansar, Z. Shiraz, H. Amir and A. G. Mayes, *Sci. Rep.*, 2024, **14**, 12714.
56 A. Evans, O. Casale, L. J. Morris, Z. R. Turner and D. O'Hare, *Macromolecules*, 2024, **57**, 10778–10791.
57 B. Neises and W. Steglich, *Angew. Chem., Int. Ed. Engl.*, 1978, **17**, 522–524.
58 L. K. Kostanski, D. M. Keller and A. E. Hamielec, *J. Biochem. Biophys. Methods*, 2004, **58**, 159–186.
59 C. J. Kay, P. D. Goring, C. A. Burnett, B. Hornby, K. Lewtas, S. Morris, C. Morton, T. McNally, G. W. Theaker, C. Waterson, P. M. Wright and P. Scott, *J. Am. Chem. Soc.*, 2018, **140**, 13921–13934.
60 Z. Gao, K. Wontor and J. V. Cizdziel, *Molecules*, 2022, **27**, 7415.
61 S. Jordans, S. Jenko-Kokalj, N. M. Kühl, S. Tedelind, W. Sendt, D. Brömme, D. Turk and K. Brix, *BMC Biochem.*, 2009, **10**, 23.
62 J. C. Prata, *Environ. Pollut.*, 2018, **234**, 115–126.
63 M. Revel, A. Châtel and C. Mouneyrac, *Curr. Opin. Environ. Sci. Health*, 2018, **1**, 17–23.
64 R. Gautam, J. Jo, M. Acharya, A. Maharjan, D. Lee, P. B. KC, C. Kim, K. Kim, H. Kim and Y. Heo, *Sci. Total Environ.*, 2022, **838**, 156089.
65 N. Jourde-Chiche, F. Fakhouri, L. Dou, J. Bellien, S. Burtey, M. Frimat, P.-A. Jarrot, G. Kaplanski, M. Le Quintrec, V. Pernin, C. Rigothier, M. Sallée, V. Fremeaux-Bacchi, D. Guerrot and L. T. Roumenina, *Nat. Rev. Nephrol.*, 2019, **15**, 87–108.
66 K. Lu, R. Qiao, H. An and Y. Zhang, *Chemosphere*, 2018, **202**, 514–520.
67 L. G. A. Barboza, L. R. Vieira, V. Branco, N. Figueiredo, F. Carvalho, C. Carvalho and L. Guilhermino, *Aquat. Toxicol.*, 2018, **195**, 49–57.
68 L. Bradney, H. Wijesekara, K. N. Palansooriya, N. Obadamudalige, N. S. Bolan, Y. S. Ok, J. Rinklebe, K.-H. Kim and M. B. Kirkham, *Environ. Int.*, 2019, **131**, 104937.
69 J. Tanaka, A. Evans, P. Gurnani, A. Kerr and P. Wilson, *Polym. Chem.*, 2020, **11**, 2519–2531.
70 L. Shang, K. Nienhaus and G. U. Nienhaus, *J. Nanobiotechnol.*, 2014, **12**, 5.
71 B. M. Webster and C. P. Lusk, *Trends Cell Biol.*, 2016, **26**, 29–39.
72 G. J. Doherty and H. T. McMahon, *Annu. Rev. Biochem.*, 2009, **78**, 857–902.

